

# Atmospheric conditions controlling extreme summertime evapotranspiration in Poland (central Europe)

Paweł Bogawski<sup>1,2</sup> · Ewa Bednorz<sup>1</sup>

Received: 19 December 2014 / Accepted: 28 October 2015 / Published online: 5 November 2015  
© The Author(s) 2015. This article is published with open access at Springerlink.com

**Abstract** Extremely high evapotranspiration may constitute a threat to agriculture and to water storage, supply, management and quality. To better understand the occurrence of high evapotranspiration, our goals were to (1) document the synoptic conditions favorable for extreme evapotranspiration and (2) determine the anomalies in the factors that directly affect extremely high evapotranspiration on a daily scale. We calculated the daily reference evapotranspiration ( $ET_0$ ; June–August, 1971–2010) for 31 stations in Poland using the FAO-56 Penman–Monteith method and identified the days with the highest  $ET_0$  values (>90th percentile). For these days, we calculated the sea level pressure (SLP), the 500 hPa geopotential heights ( $z_{500}$ ), the air temperature at 850 hPa ( $t_{850}$ ) and the amount of precipitable water. We detected a correlation between the air pressure field and high  $ET_0$  values ( $r > 0.4$ ,  $p < 0.001$ ) in northeast Poland; positive anomalies in SLP,  $z_{500}$  and  $t_{850}$  were documented on days with high  $ET_0$ . Substantial anomalies were also observed in the factors that directly affect evapotranspiration, i.e., sunshine duration and air temperature (positive) and relative humidity (negative). The conditions favorable for high  $ET_0$  events are characteristic of anticyclonic weather, so when an anticyclone center is near northeast Poland, high evapotranspiration can be expected.

**Keywords** Extreme evapotranspiration · Penman–Monteith method · Synoptic patterns · Central Europe

---

✉ Ewa Bednorz  
ewabedno@amu.edu.pl

<sup>1</sup> Department of Climatology, Faculty of Geographical and Geological Sciences, Adam Mickiewicz University, Dzięgielowa 27, 61-680 Poznan, Poland

<sup>2</sup> Laboratory of Aeropalynology, Faculty of Biology, Adam Mickiewicz University, Umultowska 89, 61-614 Poznan, Poland

## 1 Introduction

In the future, the intensity and variability of the hydrological cycle are predicted to increase, and extreme phenomena, such as floods and droughts, are likely to become more common (IPCC 2007). These extremes frequently pose economic threats, so it is essential that we further our knowledge of the entire hydrological cycle (Bosilovich and Schubert 2002). Evapotranspiration, which is defined as evaporation from the soil and transpiration from plants, is a crucial component of the hydrological cycle that may be used as a sensitive indicator of changes in the intensity of the cycle (Huntington 2006). Evapotranspiration is also one of the most important hydrological parameters for planning and managing water resources, particularly for scheduling irrigation in agriculture, so extreme evapotranspiration values (along with low precipitation) are a critical consideration from a food security perspective (Mishra and Singh 2010). Moreover, evapotranspiration is included in all hydrological water balance models and is a popular topic in many international research programs, such as the World Climate Research Programme (WCRP), the International Geosphere-Biosphere Programme (IGBP) and the International Human Dimensions Program on Global Environmental Change (Liang et al. 2008; Tabari and Talaei 2014).

The intensity of evapotranspiration is controlled by numerous meteorological factors, including solar radiation, air temperature, humidity and wind speed (i.e., Goyal 2004; Tabari and Talaei 2014), and the importance of these parameters to the variability in evapotranspiration has been repeatedly emphasized in the literature (e.g., Gong et al. 2006; Liang et al. 2008; Estevez et al. 2009). However, all of these individual meteorological and hydrometeorological parameters, including evapotranspiration, are affected by atmospheric circulation, i.e., the large-scale movement of air masses in the atmosphere. The impact of atmospheric circulation on different meteorological elements has been thoroughly studied in relation to, for example, air temperature (Xoplaki et al. 2003), precipitation (Jacobeit et al. 2009), fog (Houssos et al. 2012), snow cover and melt (Bednorz 2011), and hail (Suwała 2013). However, information about the influence of atmospheric circulation on pan evaporation and evapotranspiration remains scarce (Jalili et al. 2012).

We assume that particular pressure fields and circulation patterns over the Euro-Atlantic sector of the Northern Hemisphere result in conditions that are conducive to extreme evaporation in Poland. Furthermore, high evapotranspiration is associated with anomalies in particular meteorological variables, such as sunshine duration and the air temperature, humidity and water content in the atmosphere. Our main objective in this study is to describe the atmospheric conditions that promote extreme evapotranspiration values in Poland in the summer, namely the macroscale pressure, circulation patterns and other synoptic conditions on days with extreme evapotranspiration. The ability to predict evapotranspiration is especially important in water management as it strongly influences the supply of water for agriculture. Under the climatic conditions of Poland, where water shortages due to drought often occur during the warm season (Bonaccorso et al. 2013), predicting extreme evapotranspiration events is crucial, and such forecasts may be enhanced by understanding the atmospheric conditions that cause such events and which are examined in this study.

## 2 Materials and methods

### 2.1 Evapotranspiration model

The evapotranspiration model used in this study requires standard meteorological data, which were obtained from the Polish Institute of Meteorology and Water Management. Daily data from 31 operational meteorological stations in Poland for the summers (June–August) of 1971–2010 were employed to calculate evapotranspiration values using the model described below (Fig. 1; Table 1). A small part of the dataset was missing, especially from the beginning of the study period, and the numbers of days with data gaps are shown in Table 1. All of the data gaps were addressed using data from adjacent stations.

The Penman–Monteith FAO-56 (PMF56) method, which was developed and modified by experts from the International Commission for Irrigation and Drainage (ICID) and the Food and Agriculture Organization of the United Nations (FAO) (Allen et al. 1998), is the most commonly used method for determining reference evapotranspiration ( $ET_0$ ). The method is considered to be the standard, and it produces the most precise results when applied to various climates around the world (e.g., Trajkovic et al. 2003; Garcia et al. 2004; Sabziparvar et al. 2010; Sentelhas et al. 2010; Tabari et al. 2013). This method requires non-standard meteorological data, such as net or solar radiation, that may only be recorded at select stations, so the data are commonly unavailable. To overcome this limitation, Allen et al. (1998) proposed a set of procedures for sparse data, such as using sunshine duration as a proxy for solar radiation. These procedures, which have been calibrated for conditions in Poland, were applied in this study to calculate the daily  $ET_0$ , i.e., the evapotranspiration from well-watered, actively growing grass with a height of 0.12 m, a surface resistance of 70 Sm and an albedo of 0.23 (Allen et al. 1998).

The reference evapotranspiration was calculated with the PMF56 method as follows:

$$ET_0 = \frac{0.408\Delta(R_n - G) + \gamma \frac{900}{T_a + 273} u(e_s - e_a)}{\Delta + \gamma(1 + 0.34u)}, \tag{1}$$

where  $ET_0$  is the reference crop evapotranspiration ( $\text{mm day}^{-1}$ ),  $R_n$  is the net radiation ( $\text{MJ m}^{-2} \text{day}^{-1}$ ),  $G$  is the soil heat flux ( $\text{MJ m}^{-2} \text{day}^{-1}$ ), which is null for daily periods,  $T_a$

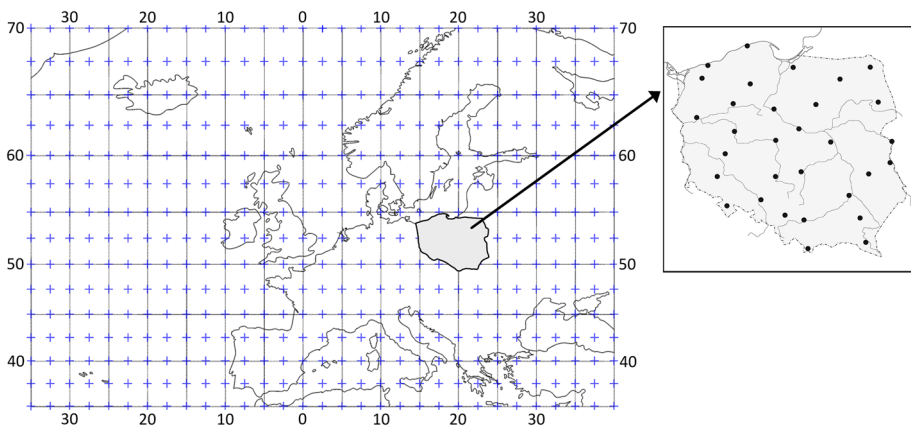


**Fig. 1** The area represented by the SLP and  $z500$  data with marked grid points and the locations of the meteorological stations used in the study

**Table 1** Description of the surface data series used to calculate reference evapotranspiration and synoptic variables used in the study

Used surface/macroscale data series	Abbreviation	Unit	Lacking data
Reference evapotranspiration	ET <sub>0</sub>	mm	–
Sunshine duration	<i>n</i> (or) SH	h	25,977 (5.7 %)
Mean air temperature at 2 m a.s.l.	<i>T<sub>a</sub></i>	°C	2
Maximum air temperature at 2 m a.s.l.	<i>T<sub>max</sub></i>	°C	3
Minimum air temperature at 2 m a.s.l.	<i>T<sub>min</sub></i>	°C	3
Precipitation	<i>P</i>	mm	1
Relative humidity	RH	%	6
Wind speed (2 m; converted from 10 m)	<i>u</i>	m s <sup>-1</sup>	703 (0.15 %)
Sea level pressure	SLP	hPa	–
500 hPa geopotential height	<i>z<sub>500</sub></i>	M	–
Mean air temperature at 850 hPa geopotential height	<i>t<sub>850</sub></i>	°C	–
Precipitable water	PW	kg m <sup>-2</sup>	–

is the average daily air temperature at a height of 2 m (°C),  $u$  is the wind speed at a height of 2 m (m s<sup>-1</sup>),  $e_s$  is the saturation vapor pressure [kPa],  $e_a$  is the actual vapor pressure (kPa),  $e_s - e_a$  is the vapor pressure deficit (kPa),  $\Delta$  is the slope of the saturation vapor pressure–temperature curve (kPa °C<sup>-1</sup>) and  $\gamma$  is the psychrometric constant (kPa °C<sup>-1</sup>).

Net and solar radiation data were lacking for almost all of the meteorological stations, so we used the procedures for estimating these two variables originally described by Allen et al. (1998). They are based on the Ångström equation (used to calculate solar radiation), which is recommended to be calibrated for local conditions (Allen et al. 1998). Therefore, we used the Ångström equation calibrated for conditions in Poland as follows (Bogawski and Bednorz 2014):

$$R_s = \left(0.094 + 0.549 \frac{n}{N}\right) R_a, \quad (2)$$

where the  $n/N$  ratio represents the relative sunshine duration (dimensionless) and  $R_a$  is the extraterrestrial radiation (MJ m<sup>-2</sup> day<sup>-1</sup>) for a particular location and day of the year.

## 2.2 Extreme ET<sub>0</sub> values

Extreme summertime evapotranspiration values were determined according to the rules of the Intergovernmental Panel on Climate Change, for which the frequency is less than or equal to 10 % (IPCC 2007). Therefore, the mean daily reference evapotranspiration values that were equal to or exceeded the 90th percentile in summer at a particular station were considered positive extremes in this station. The days when evapotranspiration exceeded the given threshold in at least half (16) of the stations in Poland were selected for further synoptic analysis, which is described in Sect. 2.3.

To determine the background conditions for the detailed analysis of the atmospheric conditions controlling extremely high evapotranspiration in Poland, we analyzed simple linear trends between the mean daily reference evapotranspiration and other

meteorological parameters ( $T_{\max}$ ,  $T_{\min}$ , SH, RH,  $P$ ) from 1971 to 2010. The data from all of the stations were averaged to calculate these trends.

### 2.3 Atmospheric circulation

To relate the occurrence of evapotranspiration extremes to synoptic conditions, the “environment-to-circulation” approach was applied. In this method, the circulation is classified according to a specific set of environmental criteria for a particular phenomenon, i.e., the evapotranspiration extremes addressed in this study (Yarnal 1993; Dayan et al. 2012). To identify the macroscale pressure patterns and circulation conditions that promote positive  $ET_0$  extremes, the mean daily sea level pressure (SLP) and 500 hPa geopotential heights ( $z500$ ) were used (Table 1). These reanalysis data were obtained from the National Centers for Environmental Prediction (NCEP)/National Center for Atmospheric Research (NCAR) (Kalnay et al. 1996). Other mesoscale meteorological conditions on the days with positive  $ET_0$  extremes were identified using air temperature at the 850 hPa level ( $t850$ ) and precipitable water (PW) data from the same source. The 850 hPa level is approximately 1500 m above the atmospheric boundary layer. At this height, the underlying surface does not affect the temperature, so  $t850$  is often used to distinguish cold and warm air masses, which are only affected by air circulation. The PW index represents the mass of water contained in a column of air above a unit surface area ( $\text{kg m}^{-2}$ ) regardless of the state of aggregation (Wibig and Siedlecki 2007). The resolution of all of the NCEP/NCAR reanalysis data used in the study is  $2.5^\circ \times 2.5^\circ$ , and area represented by the SLP and  $z500$  data with marked grid points is shown in Fig. 1.

First, the Pearson’s correlation coefficients ( $r$ ) between the daily reference evapotranspiration averaged for the 31 stations and the daily SLP values at the grid points within  $35^\circ\text{--}70^\circ\text{N}$  and  $35^\circ\text{W--}40^\circ\text{E}$  (Fig. 1) were calculated and mapped. Because of the large number of data points ( $n = 3680$ ), very low values of  $r$  were statistically significant ( $|r| = 0.055$  is statistically significant at  $p = 0.001$ ). Furthermore, composite maps of the SLP and  $z500$  means and anomalies were constructed for the days with extreme  $ET_0$  values, which were observed at more than half of the stations considered in the analysis (at least 16 stations). Additionally,  $t850$  and PW anomaly maps were constructed, and the anomalies were computed as the differences between the composite values and the 40-year summer means (June–August). All of the contour maps included in Sect. 3 were produced using Kriging with a simple linear variogram model, which is one of the most popular geostatistical gridding methods used for interpolation.

Air circulation is considered to be one of the most important factors determining weather conditions because it transports distinct air masses from various source regions. To detect the source areas of the air masses that cause extremely high evaporation in Poland, 3-day backward trajectories of air particles were constructed for select days with extreme  $ET_0$  using the NOAA Hybrid Single Particle Lagrangian Integrated Trajectory (HYSPLIT) model (Rolph 2012; Draxler and Rolph 2012). HYSPLIT is a commonly used trajectory model developed by the National Oceanic and Atmospheric Administration’s (NOAA) Air Resources Laboratory (ARL). HYSPLIT uses archived three-dimensional meteorological fields generated from observations and short-term forecasts, and it can be run to generate forward or backward trajectories using several available meteorological data archives. Back trajectory analyses use interpolated or modeled meteorological fields to estimate the most likely paths over geographical areas that provide air to a destination area at a given time. Essentially, the method follows a parcel of air backward in hourly steps for a specified length of time. The backward trajectories were computed with the NCEP/NCAR

reanalysis data available from the ARL. The analysis of the air trajectories substantially added to the information obtained from the synoptic maps and made it possible to identify the direction of air flows on the days with extreme evapotranspiration.

Finally, anomaly maps of the main meteorological variables, such as  $ET_0$ ,  $T_{max}$ , SH and RH, were constructed for the days with extreme  $ET_0$  in at least 16 stations (see the explanations in Sect. 2.2). Anomalies were computed as the differences between the composite values and the 40-year summer means (June–August).

### 3 Results

#### 3.1 Mean and extreme reference evapotranspiration values in summer

The mean evapotranspiration values for summer were highest in the central part of the country and extended zonally from west to east, where they exceeded 2.9 mm (Fig. 2, left). For this study, the days with extreme  $ET_0$  values were selected separately for each station. The values of the established 90th percentile ranged from 4.6 mm in central Poland to 3.5 in southern Poland; the spatial distribution of these values was similar to that of the mean evapotranspiration values (Fig. 2, right).

The synoptic analysis only took the days when  $ET_0$  exceeded the 90th percentile in at least 16 stations into consideration, which amounted to 410 days (out of total number of 3680 summer days used in the analysis). Of those, 210 days occurred in July, 169 days in June and 31 days in August. Most of the extreme  $ET_0$  days (68 %) were observed in the last two decades (1990–2010).

#### 3.2 Multiannual changes in the selected meteorological parameters

The linear trends in the mean daily  $ET_0$  and the associated meteorological factors were calculated (Fig. 3), and the mean daily reference evapotranspiration in summer increased

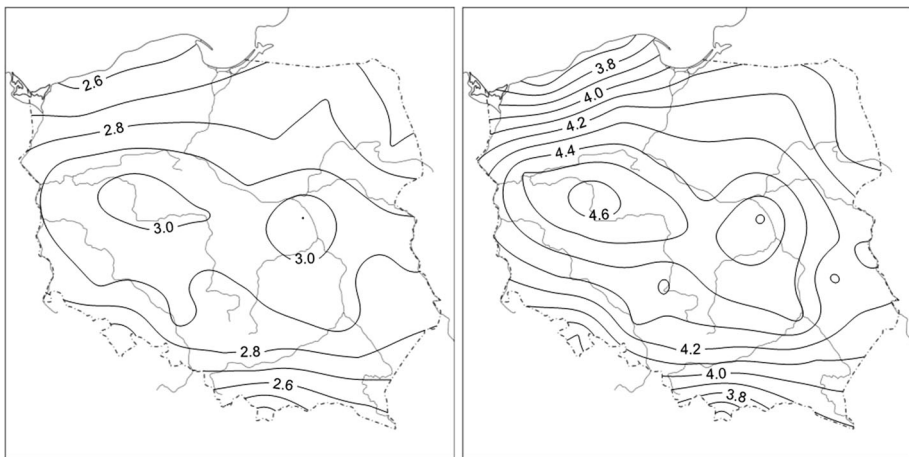
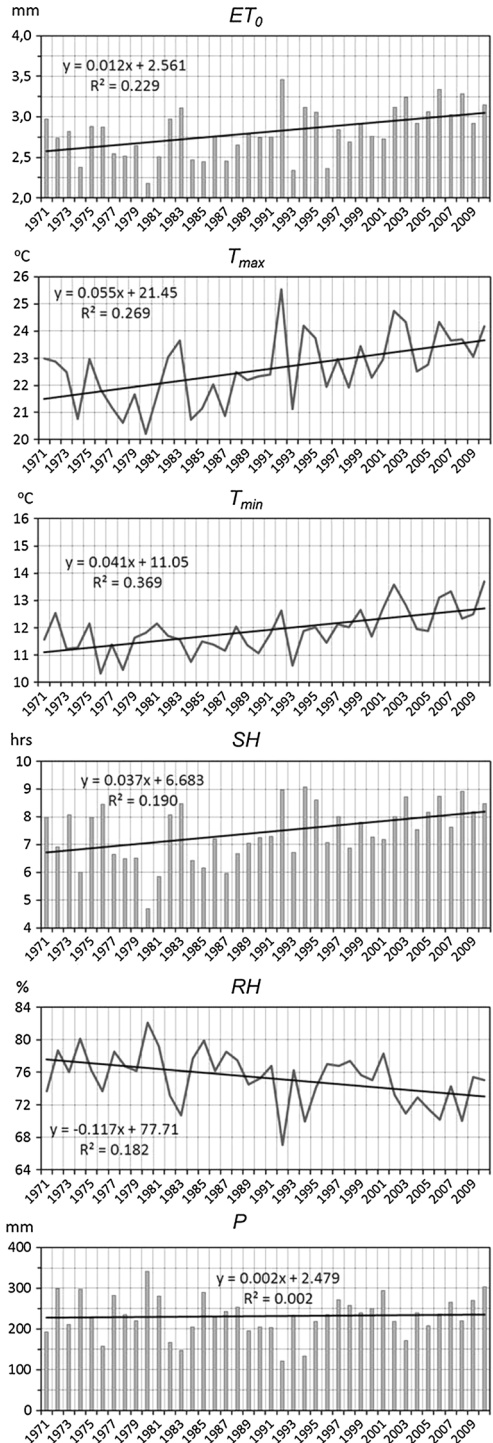


**Fig. 2** Mean daily evapotranspiration  $ET_0$  (left) and 90th percentile (right) values for the summer season (June–August) in Poland (in mm). Data for the years 1971–2010

**Fig. 3** Multiannual course of the selected meteorological parameters with trend lines and equations averaged for 31 meteorological stations in Poland for summer (Jun–Aug).  $ET_0$ , reference evapotranspiration (mm);  $T_{max}$ , daily maximum temperature (°C);  $T_{min}$ , daily minimum temperature (°C); SH, sunshine hours (h); RH, relative humidity (%);  $P$ , total summer precipitation (mm)



overall from 1971 to 2010 (0.12 mm/decade,  $p < 0.01$ ). The highest evapotranspiration value was recorded in the summer of 1992 (mean daily value of 3.5 mm) and was accompanied by very low precipitation (122 mm) and long-duration mean daily sunshine (approximately 9 h). After 2002, mean daily values exceeding 3 mm occurred nearly every summer.

Statistically significant changes were also detected in the meteorological parameters that strongly influence evapotranspiration, such as the maximum daily air temperature (0.55 °C/decade;  $p < 0.01$ ), minimum daily air temperature (0.41 °C/decade;  $p < 0.01$ ), mean daily sunshine duration (0.37 h/decade;  $p < 0.01$ ) and relative humidity (−1.17 %/decade;  $p < 0.01$ ). The summer precipitation totals exhibited year-to-year variability, but the trends were not statistically significant.

### 3.3 Synoptic conditions on the days with extreme evapotranspiration

The mean SLP was highest (>1024 hPa) southeast of the Azores, and it gradually decreased toward the north. A low-pressure center (<1000 hPa) was located over the north Atlantic southwest of Iceland. A smaller pressure gradient was observed over eastern Europe than over the Atlantic (Fig. 4a, solid lines).

$z_{500}$  is often used to study upper-level flow because it is strongly related to surface conditions. In summer, the mean  $z_{500}$  declined from the southwest (5700 m over the Azores) to the north (5500 m over the northern Atlantic) (Fig. 4a, dashed lines). Such patterns cause westerly and southwesterly airflows in both the low and middle troposphere, particularly over the study area in summer.

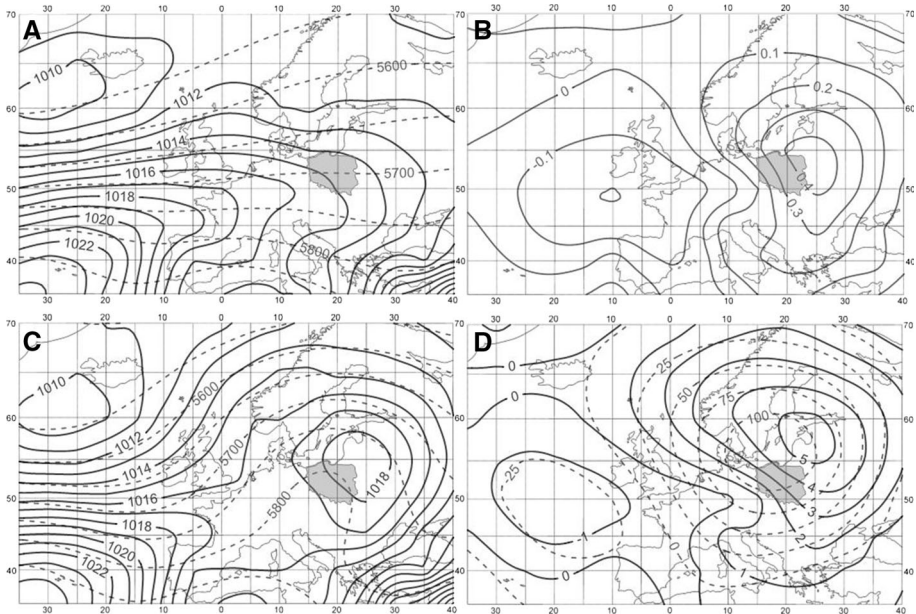


**Fig. 4** Mean sea level pressure (SLP) in hPa (solid lines) and height of geopotential level of 500 hPa ( $z_{500}$ ) in gpm (dashed lines) in summer (a); the correlation coefficient between the SLP in the grid points and the  $ET_0$  (b); composite map (c) and anomaly map (d) of SLP (solid lines) and  $z_{500}$  (dashed lines) for the days with extreme evapotranspiration in Poland

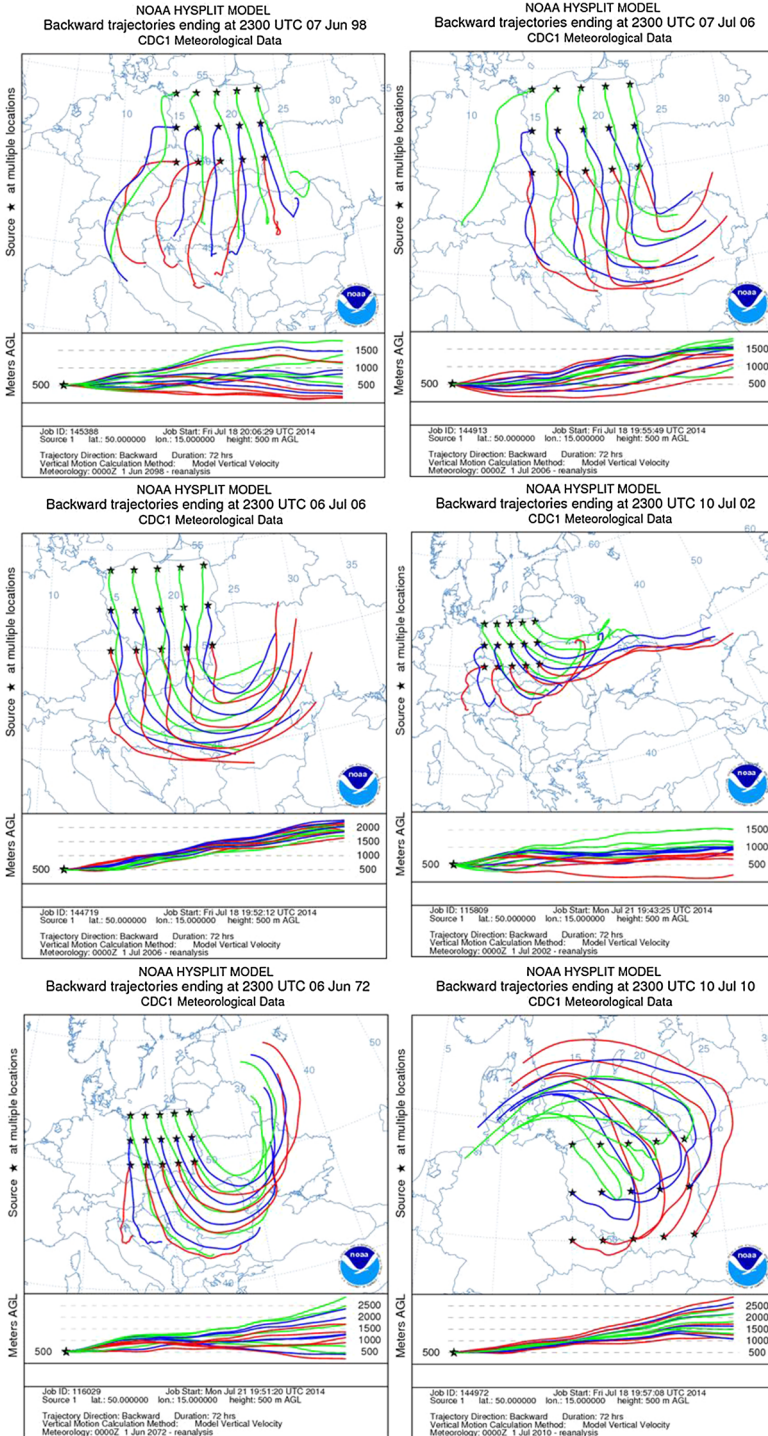


First, to relate the occurrence of evapotranspiration extremes to synoptic conditions, the correlation coefficients between the daily reference evapotranspiration averaged for 31 stations and the daily values of the SLP at each grid point within  $35^{\circ}$ – $70^{\circ}$ N and  $35^{\circ}$ W– $40^{\circ}$ E were computed and mapped (Fig. 4b). The 0.1 and  $-0.1$  contour lines bound the areas of statistically significant relationships ( $p > 0.001$ ). Second, SLP and  $z500$  composite and anomaly maps for the days with extreme  $ET_0$  were constructed (Fig. 4c, d). The correlation map (Fig. 4b) shows the location of the “centers of action”, namely the centers of low- and high-pressure systems’ which govern the intensity of  $ET_0$  in Poland. The correlation field indicates the strongest relationships between evapotranspiration and SLP in the eastern part of the study area, particularly northeast of Poland ( $r > 0.4$ ), which means that high values of  $ET_0$  in Poland are associated with high SLP values in this area and low values of  $ET_0$  are accompanied with low-pressure systems, which locate northeast of Poland. This is also indicated in Figs. 4c and d (solid lines). The SLP in the area northeast of Poland exceeds 1018 hPa ( $>5$  hPa anomalies) in the days of extreme  $ET_0$ , and positive anomalies in  $z500$  occurred simultaneously over this anticyclone, which confirms the presence of warm air masses with low densities. An evaluation of the individual days with extreme evapotranspiration showed that the locations with the most pronounced positive SLP anomalies varied from the eastern to the northeastern parts of the study area. These pressure patterns induce an inflow of warm air masses from the eastern sector (NE, E, and SE) in the lower troposphere. Simultaneously, advection of tropical air masses from the southwest occurs in the upper troposphere (500 hPa).

The 72-h backward trajectories of the air parcels for the selected days with extreme evapotranspiration confirmed the northeastern, eastern or southeastern direction of the air flow into central Europe (Fig. 5). However, when the pressure field over Europe was indistinct, with a weak anticyclone and a small pressure gradient over the eastern part of the continent, the northward movement of the air masses was slow, as shown by the backward trajectory ending on June 7, 1998. However, the strong anticyclone indicated dynamic movement of the air, and southern Scandinavia was identified as the source region of the air masses (backward trajectory ending on July 10, 2010). Most of the trajectories showed downward movement of the air masses (from 1500–2500 m AGL to 500 m AGL), which is typical of a high-pressure system.

The described directions of the air flows caused positive anomalies in  $t850$  over most of the continent; these anomalies were highest ( $>5$  °C) over western Poland and Germany (Fig. 6a). Additionally, positive PW anomalies were observed over Western Europe (Fig. 6b). According to the Clausius–Clapeyron equation, higher than normal water content in the atmosphere is related to high temperatures, but in eastern Poland, the PW anomalies were negative due to hot but dry continental air advection from the east.

In summer, the influx of air masses from the east and southeast to central Europe caused positive  $ET_0$  extremes as well as positive anomalies in the meteorological factors controlling  $ET_0$  (Fig. 7). On days with extreme  $ET_0$  (1.3–2 mm higher than the station averages), large positive  $T_{\max}$  anomalies were observed that exceed  $4.5$  °C in most of Poland and amount to  $-7.5$  °C in the central-western part of the country. This means that  $T_{\max}$  exceeded  $30$  °C in western Poland on the days with positive  $ET_0$  extremes. High values of  $ET_0$  are also accompanied by very high values of SH, which may exceed 13.5 h in central Poland (SH anomalies  $>6$  h). Despite the positive PW anomalies described previously and despite high vapor pressure during the days with extreme evapotranspiration, the RH is lower than the summer average (81–72 %, depending on the region) by 10 % in the most of Poland, due to the high air temperatures.



◀ **Fig. 5** The 72-h back trajectories for the selected days with extreme evapotranspiration in Poland. Colors stand for back trajectories generated for the points in different latitudes: green 53°N, blue 52°N, red 50°N

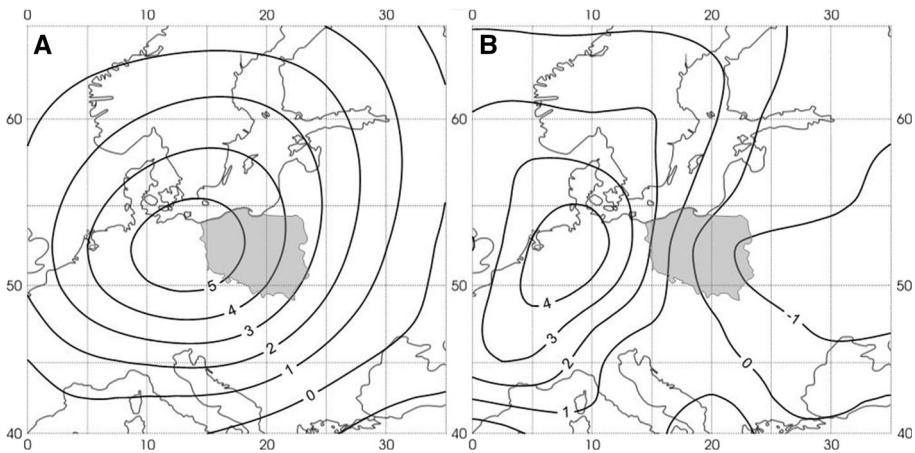


**Fig. 6** Anomaly maps of air temperature at geopotential level 850 hPa ( $t_{850}$ ) in °C (a) and precipitable water (PW) in  $\text{kg m}^{-2}$  (b) for the days with extreme evapotranspiration in Poland

## 4 Discussion

The  $ET_0$  values estimated using the Penman–Monteith FAO-56 method calibrated for Poland increased during the study period (1971–2010). This result is similar to those obtained in southern Europe, in Romania (Croitoru et al. 2013) and in Spain (Vicente-Serrano et al. 2014). Additionally, a recent study of changes in  $ET_0$  during the growing season (April–September) in Poland found a clear increase in  $ET_0$  (Łabędzki et al. 2014).

The  $ET_0$  values are sensitive to changes in basic climate variables such as air temperature, humidity, solar radiation and wind speed (Gong et al. 2006; Valiantzas 2013). An increase in air temperature and solar radiation increases  $ET_0$ , whereas an increase in air humidity decreases  $ET_0$  when other factors are unchanged (Goyal 2004). The influence of those factors depends on the climate type;  $ET_0$  is most sensitive to sunshine hours and thus solar radiation, as well as air humidity in humid climates (Xu et al. 2006; Tabari and Talaei 2014). These findings seem to be confirmed by this study as sunshine duration increased and air humidity decreased with the increase in  $ET_0$  in recent decades. In turn, the influence of air temperature on  $ET_0$  in humid climates is not so distinct as in arid climates (Tabari and Talaei 2014). However, wind speed might play a dual role. High wind speed may enhance the removal of water particles from the surface of the water and thus increase  $ET_0$ , but it may also cause a decrease in the transmissivity of the atmosphere, which would limit solar radiation and thus decrease  $ET_0$  (Goyal 2004). However, wind speed is generally considered to be a minor influence on  $ET_0$  changes in humid climates. All of the meteorological elements mentioned are strongly influenced by air circulation, and this study identified the relevant features of the circulation patterns and synoptic conditions responsible for extreme values of  $ET_0$  in Poland.

We found that anticyclonic pressure patterns result in the synoptic conditions associated with the highest  $ET_0$  values. Anticyclones, i.e., high-pressure systems with clockwise descending air flow (Northern Hemisphere), may form over the Baltic Sea and to the

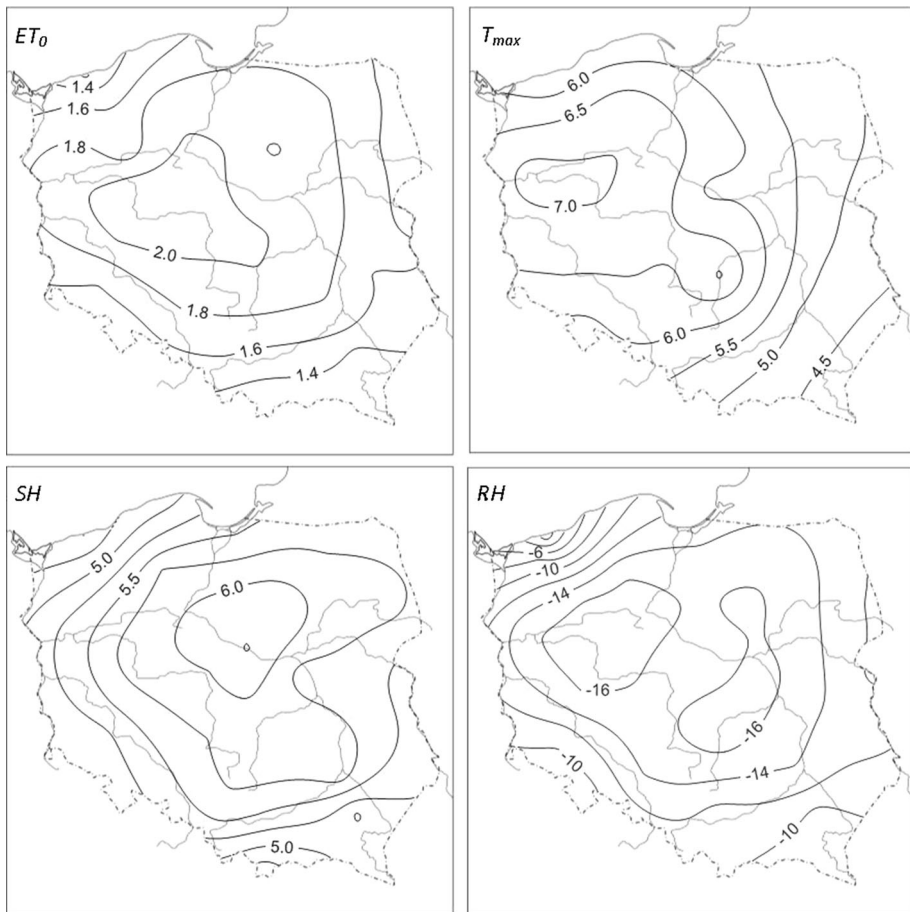


**Fig. 7** Anomalies in selected meteorological parameters on the days with extreme evapotranspiration in Poland;  $ET_0$ , reference evapotranspiration (mm);  $T_{max}$ , daily maximum temperature ( $^{\circ}C$ ); SH, sunshine hours (h); RH, relative humidity (%)

southeast; these systems are detectable from sea level to the middle troposphere. This anticyclonic pressure pattern is associated with warm and dry continental air, clear skies, and a strong solar energy flux. An increase in solar radiation enhances the surface energy balance and increases the temperature, which leads to extreme  $ET_0$  values.

Midlatitude summer anticyclones are known to generate extreme evapotranspiration and other extreme weather conditions, and these systems are mainly responsible for the heat waves and persistent droughts in Europe (Fink et al. 2004; Rebetez et al. 2006). For example, the importance of persistent anticyclonic conditions in the development of the 2003 heat wave over Europe was described by Black et al. (2004). Similar conditions caused the 1992 and 1994 heat waves over Prague (Kyselý 2010) and the southern coast of the Baltic Sea (Tomczyk and Bednorz 2014). According to Ustrnul et al. (2010) and Wibig (2007), the highest temperatures in Poland are associated with anticyclones without distinct advection. According to Wibig (2007), such temperatures are associated with positive anomalies in the 700 hPa geopotential level and southeasterly flow at this height, which

usually transports hot and dry air in summer. Midlatitude summer anticyclones are also associated with high solar radiation, which is related to high evapotranspiration.

A significant increase in the mean daily values of the summer  $ET_0$  in Poland during 1971–2010 was recognized using simple linear trend analysis, so the increase in  $ET_0$  may indicate increasing intensity in the hydrological cycle (Huntington 2006), which can be linked to recent climate change (Goyal 2004; Gong et al. 2006; Irmak et al. 2012; Huo et al. 2013). In addition to anthropogenic forcings, natural processes—mainly air circulation—are also widely linked to climate change (Kysely and Domonkos 2006; Werner et al. 2000). An increasing persistence of the various types of circulation, including anticyclonic patterns, has recently been reported (Werner et al. 2000; Kysely and Domonkos 2006). Along with the increasing frequency of blocking anticyclonic systems over Europe in recent decades, the number of low-pressure systems south of 55°N has decreased (Leckebusch and Ulbrich 2004). Therefore, the increasing evapotranspiration observed in Poland may be partly linked to the upward trend in the frequency and persistence of anticyclonic circulations. In this case, extreme  $ET_0$  events have the potential to occur more frequently in the future.

## 5 Conclusions

The extremely high daily evapotranspiration values (90th percentile) observed in summer (June–August) in Poland during 1971–2010 ranged from 3.7 mm in northern and southern Poland to 4.6 mm in central Poland. The synoptic conditions on days with extreme evapotranspiration were compared with the average synoptic patterns during summer. This study demonstrated that the most favorable conditions for high  $ET_0$  in Poland (central Europe) were elevated SLP (5 hPa anomalies northeast of Poland), elevated  $z500$  (100 m anomalies over the southern Baltic Sea) and elevated  $t850$  ( $>5$  °C anomalies over Germany and western Poland). These synoptic patterns are typical of anticyclonic circulations and are accompanied by strong meteorological factors that directly control  $ET_0$ , including  $T_{max}$ ,  $T_{min}$  and  $n$  as well as low values of RH. The increases detected in the aforementioned factors (apart from RH, which decreased) coincided with increases in  $ET_0$ , and these changes may result from the increase in the frequency of anticyclonic circulations in central Europe. However, the evapotranspiration tendency in this region requires more detailed analysis.

**Acknowledgment** This work was funded by the Polish National Science Center within the framework of Project No. 2011/01/N/ST10/05954. The first author received a scholarship from the Foundation of the Adam Mickiewicz University in Poznan for 2014/2015. We thank the Institute of Meteorology and Water Management for providing the meteorological data.

**Open Access** This article is distributed under the terms of the Creative Commons Attribution 4.0 International License (<http://creativecommons.org/licenses/by/4.0/>), which permits unrestricted use, distribution, and reproduction in any medium, provided you give appropriate credit to the original author(s) and the source, provide a link to the Creative Commons license, and indicate if changes were made.

## References

Allen RG, Pereira LS, Raes D, Smith M (1998) Crop evapotranspiration. Guidelines for computing crop water requirements—FAO Irrigation and drainage paper 56. FAO, Rome

- Bednorz E (2011) Synoptic conditions of the occurrence of snow cover in central European lowlands. *Int J Climatol* 31(8):1108–1118
- Black E, Blackburn M, Harrison G, Hoskins B, Methven J (2004) Factors contributing to the summer 2003 European heatwave. *Weather* 59:217–223
- Bogawski P, Bednorz E (2014) Comparison and validation of selected evapotranspiration models for conditions in Poland (central Europe). *Water Resour Manag* 28(14):5021–5038
- Bonaccorso B, Peres DJ, Cancelliere A, Rossi G (2013) Large scale probabilistic drought characterization over Europe. *Water Resour Manag* 27:1675–1692
- Bosilovich MG, Schubert SD (2002) Water vapor tracers as diagnostics of the regional hydrologic cycle. *J Hydrometeorol* 3:149–165
- Croitoru A-E, Piticar A, Dragota CS, Burada C (2013) Recent changes in reference evapotranspiration in Romania. *Global Planet Change* 111:127–137
- Dayan U, Tubia A, Levy I (2012) On the importance of synoptic classification methods with respect to environmental phenomena. *Int J Climatol* 32:681–694
- Draxler RR, Rolph GD (2012) HYSPLIT (HYbrid Single-Particle Lagrangian Integrated Trajectory) model access via NOAA ARL READY website. <http://ready.arl.noaa.gov/HYSPLIT.php>. NOAA Air Resources Laboratory, Silver Spring, MD
- Estevez J, Gavilan P, Berengena J (2009) Sensitivity analysis of a Penman–Monteith type equation to estimate reference evapotranspiration in southern Spain. *Hydrol Process* 23:3342–3353
- Fink A, Brücher T, Krüger A, Leckebusch G, Pinto J, Ulbrich U (2004) The 2003 European summer heatwaves and drought—synoptic diagnosis and impacts. *Weather* 59:209–216
- Garcia M, Raes D, Allen R, Herbas C (2004) Dynamics of reference evapotranspiration in the Bolivian highlands (Altiplano). *Agric For Meteorol* 125:67–82
- Gong L, Xu C-Y, Chen D, Halldin S, Chen YD (2006) Sensitivity of the Penman–Monteith reference evapotranspiration to key climatic variables in the Changjiang (Yangtze River) basin. *J Hydrol* 329:620–629
- Goyal RK (2004) Sensitivity of evapotranspiration to global warming: a case study of arid zone of Rajasthan (India). *Agric Water Manag* 69:1–11
- Houssos EE, Lolis CJ, Gkikas A, Hatzianastassiou N, Bartzokas A (2012) On the atmospheric circulation characteristics associated with fog in Ioannina, north-western Greece. *Int J Climatol* 32(12):1847–1862
- Huntington TG (2006) Evidence for intensification of the global water cycle: review and synthesis. *J Hydrol* 319:83–95
- Huo Z, Dai X, Feng S, Kang S, Huang G (2013) Effect of climate change on reference evapotranspiration and aridity index in arid region of China. *J Hydrol* 492:24–34
- IPCC (2007) Climate change 2007: synthesis report. In: Pachauri RK, Reisinger A (eds) Contribution of working groups I, II and III to the fourth assessment report of the intergovernmental panel on climate change, Switzerland, Geneva
- Irmak S, Kabenge I, Skaggs KE, Mutiibwa D (2012) Trend and magnitude of changes in climate variables and reference evapotranspiration over 116-yr period in the Platte River Basin, central Nebraska–USA. *J Hydrol* 420–421:228–244
- Jacobeit J, Rathmann J, Philipp A, Jones PD (2009) Central European precipitation and temperature extremes in relation to large-scale atmospheric circulation types. *Meteorol Z* 18(4):397–410
- Jalili S, Kirchner I, Livingstone DM, Morid S (2012) The influence of large-scale atmospheric circulation weather types on variations in the water level of Lake Urmia, Iran. *Int J Climatol* 32(13):1990–1996
- Kalnay E, Kanamitsu M, Kistler R, Collins W, Deaven D, Gandin L, Iredell M, Saha S, White G, Woollen J, Zhu Y, Leetmaa A, Reynolds R, Chelliah M, Ebisuzaki W, Higgins W, Janowiak J, Mo KC, Ropelewski C, Wang J, Jenne R, Joseph D (1996) The NMC/NCAR 40-year reanalysis project. *Bull Am Meteorol Soc* 77:437–471
- Kysely J (2010) Recent severe heat waves in central Europe: how to view them in a long-term prospect? *Int J Climatol* 30:89–109
- Kysely J, Domonkos P (2006) Recent increase in persistence of atmospheric circulation over Europe: comparison with long-term variations since 1881. *Int J Climatol* 26:461–483
- Łabędzki L, Bąk B, Smarzyńska K (2014) Spatio-temporal variability and trends of Penman–Monteith reference evapotranspiration (FAO-56) in 1971–2010 under climatic conditions of Poland. *Pol J Environ Stud* 23(6):2083–2091
- Leckebusch GC, Ulbrich U (2004) On the relationship between cyclones and extreme windstorms over Europe under climate change. *Global Planet Change* 44:181–193
- Liang L, Li L, Zhang L, Li J, Li B (2008) Sensitivity of Penman–Monteith reference crop evapotranspiration in Tao'er River Basin of northeastern China. *Chin Geogr Sci* 18(4):340–347
- Mishra AK, Singh VP (2010) A review of drought concepts. *J Hydrol* 391(1–2):202–216

- Rebetez M, Dupont O, Giroud M (2006) An analysis of the July 2006 heatwave extent in Europe compared to the record year of 2003. *Theor Appl Climatol* 95(1–2):1–7
- Rolph GD (2012) Real-time Environmental Applications and Display sYstem (READY) website. <http://ready.arl.noaa.gov>. NOAA Air Resources Laboratory, Silver Spring, MD
- Sabziparvar AA, Tabari H, Aeini A, Ghafouri M (2010) Evaluation of class A pan coefficient models for estimation of reference crop evapotranspiration in cold-semi arid and warm arid climates. *Water Resour Manag* 24(5):909–920
- Sentelhas P, Gillespie T, Santos E (2010) Evaluation of FAO Penman–Monteith and alternative methods for estimating reference evapotranspiration with missing data in Southern Ontario, Canada. *Agric Water Manag* 97:635–644
- Suwala K (2013) The influence of atmospheric circulation on the occurrence of hail in the North German Lowlands. *Theor Appl Climatol* 112(3–4):363–373
- Tabari H, Talaei PH (2014) Sensitivity of evapotranspiration to climatic change in different climates. *Global Planet Change* 115:16–23
- Tabari H, Grismer ME, Trajkovic S (2013) Comparative analysis of 31 reference evapotranspiration methods under humid conditions. *Irrig Sci* 31:107–117
- Tomczyk AM, Bednorz E (2014) Heat and cold waves on the southern coast of the Baltic Sea. *Baltica* 27(1):45–53
- Trajkovic S, Todorovic B, Stankovic M (2003) Forecasting reference evapotranspiration by artificial neural networks. *J Irrig Drain Eng* 129(6):454–457
- Ustrnul Z, Czekierda D, Wypych A (2010) Extreme values of air temperature in Poland according to different atmospheric circulation classifications. *Phys Chem Earth* 35:429–436
- Valiantzas J (2013) Simplified forms for the standardized FAO-56 Penman–Monteith reference evapotranspiration using limited weather data. *J Hydrol* 505:13–23
- Vicente-Serrano SM, Lopez-Moreno J, Beguería S, Lorenzo-Lacruz J, Sanchez-Lorenzo A, García-Ruiz JM, Azorin-Molina C, Morán-Tejada E, Revuelto J, Trigo R, Coelho F, Espejo F (2014) Evidence of increasing drought severity caused by temperature rise in southern Europe. *Environ Res Lett* 9:044001
- Werner PC, Gerstengarbe F-W, Fraedrich K, Oesterle H (2000) Recent climate change in the North Atlantic/European sector. *Int J Climatol* 20:463–471
- Wibig J (2007) Fale ciepła i chłodu w środkowej Polsce na przykładzie Łodzi (Waves of warmth and coldness in Central Poland on the example of Łódź). *Acta Univ Lodz Folia Geogr Phys* 8:27–61 (**in Polish**)
- Wibig J, Siedlecki M (2007) Przestrzenny i czasowy rozkład zawartości wody opadowej [Spatial and temporal distribution of precipitable water content]. In: Piotrowicz K, Twardosz R (eds) *Wahania klimatu w różnych skalach przestrzennych i czasowych* [Variability of climate in different spatial and temporal scales]. Instytut Geografii i Gospodarki Przestrzennej Uniwersytetu Jagiellońskiego, Kraków, pp 195–202 (**in Polish**)
- Xoplaki E, González-Rouco JF, Luterbacher J, Wanner H (2003) Mediterranean summer air temperature variability and its connection to the large-scale atmospheric circulation and SSTs. *Clim Dyn* 20(7–8):723–739
- Xu C-Y, Gong L, Jiang T, Chen D, Singh VP (2006) Analysis of spatial distribution and temporal trend of reference evapotranspiration and pan evaporation in Changjiang (Yangtze River) catchment. *J Hydrol* 327:81–93
- Yarnal B (1993) *Synoptic climatology in environmental analysis*. Belhaven Press, London